JOURNAL OF MASS SPECTROMETRY
J. Mass Spectrom. 2006; **41**: 659–669
Published online 10 April 2006 in Wiley InterScience (www.interscience.wiley.com). DOI: 10.1002/jms.1025

JMS

Radical cation formation in characterization of novel C_3-symmetric disks and their precursors by matrix-assisted laser desorption/ionization time-of-flight mass spectrometry

Xianwen Lou,* Kelly P. van den Hout, Michel H. C. J. van Houtem, Joost L. J. van Dongen, Jef A. J. M. Vekemans and E. W. Meijer

Laboratory of Macromolecular and Organic Chemistry, Eindhoven University of Technology, P.O. Box 513, 5600 MB Eindhoven, The Netherlands

Received 17 November 2005; Accepted 16 February 2006

Four C_3-symmetrical tris(dipeptide) disks and their precursors were characterized using matrix-assisted laser desorption/ionization time-of-flight mass spectrometry (MALDI TOF MS). The C_3-symmetrical disks were based on a benzene-1,3,5-triscarboxamide core extended by oligopeptides with trialkoxyanilide tails. The results indicate that MALDI TOF MS is a powerful and straightforward analytical technique for characterizing C_3-symmetrical disks and their precursors. Clear (pseudo)-molecular ion peaks could readily be identified. It is remarkable that strong radical ion signals were observed for all the compounds, including the anilines that were expected to be protonated prior to laser irradiation using acidic MALDI matrixes. Possible mechanisms for radical ion formation were investigated with the employment of radical scavengers, with various matrixes and with direct laser desorption/ionization (LDI). Most likely the radicals are formed by losing one electron from the aniline nitrogen and stabilized by conjugation through the phenyl ring. It appears that direct photo/thermal ionization of analytes is an important route for the radical ion formation of the compounds with trialkoxy aniline/anilide groups. Copyright © 2006 John Wiley & Sons, Ltd.

KEYWORDS: matrix-assisted laser desorption/ionization time-of-flight mass spectrometry; radical cation; C_3-symmetric disk; aniline; photo/thermal ionization

INTRODUCTION

Several C_3-symmetrical disks synthesized in our group are based on a benzene triscarboxamide core and are capable of associating in supramolecular multivalent helical stacks.[1–5] The dynamically ordered helix, which is one of the basic structural motifs in proteins, has found new applications in the fields of biology, pharmacy and material sciences.[6–8] In the self-assembly process of the disk-shaped molecules, hydrogen bonding, $\pi - \pi$ interactions as well as solvophobic effects play important roles. An appealing property of these C_3-symmetrical disks is that they can reversibly form helical stacks consisting of hundreds of molecules both in the solid state and in solution.

In many chemistry laboratories, characterization using mass spectrometry (MS) has become imperative. This is especially the case after the advent of the soft ionization techniques of matrix-assisted laser desorption/ionization (MALDI) and electrospray ionization (ESI).[9–12] Since its introduction in the late 1980s, matrix-assisted laser desorption/ionization time-of-flight mass spectrometry (MALDI TOF MS) has found numerous applications in many areas ranging from biomedical compounds to synthetic polymers.[13–15] In this work, four novel C_3-symmetrical disks together with their precursors, all with trialkoxy aniline/anilide tails, were analyzed using MALDI TOF MS.

One intriguing phenomenon observed in our experiments is the emergence of strong radical ion peaks of analytes that should be protonated in the condensed phase prior to laser irradiation (see below). In MALDI TOF MS, usually not radical ions, but protonated and/or metal ion adducts were detected for a great majority of samples. Actually, only a limited number of compounds with low ionization potential (IP) values could yield radical ions in MALDI.[16–21]

It is well known that ionization in MALDI is a very complicated process happening in the timescale of a few nanoseconds. Many parameters could affect the outcome of this process and, hence, the final ion species and their abundance in an MS spectrum. A number of ionization models have been developed aiming to improve the knowledge of how the analyte ions are formed.[18,22–25] In most of the models, it is assumed that photoionized

*Correspondence to: Xianwen Lou, Laboratory of Macromolecular and Organic Chemistry, Eindhoven University of Technology, P.O. Box 513, 5600 MB Eindhoven, The Netherlands.
E-mail: x.w.lou@tue.nl

matrix radical ions are profuse in the MALDI plume and a key to ion generation. Interestingly though, most of the models focused mainly on the generation of protonated analyte ions or metal ion adducts. Fewer investigations have been undertaken on the analyte radical ions, probably because they are less frequently observed in MALDI. For the analyte radicals, McCarley *et al*.[17] proposed an electron-transfer ionization mechanism, which could satisfactorily explain radical ionization of analytes that cannot logically undergo proton transfer reactions. In this mechanism, they argued that matrixes absorbed the laser radiation and became photoionized. Analyte radical ions were then produced by molecule–ion reactions of neutral analytes with matrix radical ions. Unfortunately, this mechanism could not explain most of our experimental results.

The aim of this paper is twofold: Firstly, MALDI TOF MS was used to analyze the C_3-symmetrical disks and their precursors. It is remarkable that clear radical ions were observed for all the compounds analyzed. Secondly, possible mechanisms for the radical ion generation were investigated by a series of experiments, including the addition of radical scavengers, the employment of an inorganic particle matrix, the use of direct laser desorption ionization (LDI) and the introduction of suppression effects of K^+ with the addition of excessive amount of K_2CO_3. On the basis of the experimental results, possible mechanisms for the radical ion formation are discussed.

EXPERIMENTAL

The structures of compounds studied are depicted in Fig. 1. The disk-shaped molecules were synthesized via a convergent approach.[1,26,27] First, a trialkoxy amine was incorporated into an oligopeptide fragment. In case an achiral glycine is adjacent to the trialkoxy moiety, the Boc-protected dipeptide was directly linked to the trialkoxyamine using *O*-(benzotriazol-1-yl)-*N*,*N*,*N*′,*N*′-tetramethyluronium hexafluorophosphate (HBTU) as a coupling agent. When a chiral phenylalanine is present next to the trialkoxy moiety, step-by-step coupling of the Boc-protected amino acids is required to prevent racemization. The amine-terminated conjugates were obtained after removal of the protecting Boc-group with TFA followed by a basic work-up. Finally, disk-shaped molecules were obtained via coupling of the amine-terminated dipeptide anilines to 1,3,5-benzenetricarbonyl trichloride using triethylamine as the base.

Four organic and one inorganic matrixes were used in this work. α-Cyano-4-hydroxy cinnamic acid (CHCA) and 2,5-dihydroxybenzoic acid (DHB) were obtained from Fluka (Buchs, Switzerland), and dithranol and ZnO (nanopowder, particle size <1 μm) from Aldrich (Steinheim, Germany). 2-[(2*E*)-3-(4-*tert*-Butylphenyl)-2-methylprop-2-enylidene] malononitrile (DCTB) was synthesized according to Ulmer *et al*.,[28] who used it for the MALDI TOF MS analysis of some substituted fullerenes. Butylated hydroxytoluene (BHT) was received from Aldrich, and the other radical scavenger, *N*, *N*, *N*′,*N*′-tetraphenyl-1,4-benzenediamine (NTPBDA), was kindly provided by Dr M. M. Wienk.

The MALDI TOF MS measurements were performed with a Voyager-DE Pro (PerSeptive Biosystems) instrument equipped with a 337-nm nitrogen laser, capable of executing both linear and reflector modes. The accelerating voltage was held at 20 kV for all experiments. Mass spectra were acquired in the reflector mode by summing spectra from 100 selected laser shots and calibrated with oligothiophenes of known masses. For the experiments with organic matrixes, matrix solutions were freshly prepared in tetrahydrofuran (THF) at a concentration of about 20 mg/ml, and sample solutions at about 2 mg/ml. The sample solution and matrix solution were mixed 1/1 in an Eppendorf tube, and about 0.5 μl of the mixed solution was pipetted onto a stainless steel MALDI target plate. Samples prepared in this way yielded a molar ratio of analyte to matrix of around 1 : 50. Unless noted otherwise, this ratio is used throughout this article. This is because similar results were observed for radical cation formation in a wide range of molar ratios from 1 : 10 to 1 : 1000 and a ratio of 1 : 50 was convenient for sample preparation. When a radical scavenger was used, the scavenger solution (also in THF at about 20 mg/ml) was combined with the mixed solution of sample and matrix prior to pipetting. The mole ratios of matrix : scavenger : analyte were at about 50 : 50 : 1 for BHT and 50 : 25 : 1 for NTPBDA. In the experiments with the ZnO matrix, the inorganic particle was dispersed with methanol (20 mg/ml) in an ultrasonic bath for 30 min. The solution was then spotted on the plate. After evaporation of methanol, about 0.5 μl of the sample solution was deposited on top of the inorganic matrix.

ESI MS measurements were carried out with an LCQ Deca XP MAX instrument (Thermo Finnigan, San Jose, CA) equipped with an ion trap. A MALDI solution (a mixed solution of sample and the CHCA matrix, as above) was first diluted by about 100 times with THF. The diluted solution (5 μl) was then directly introduced into the ESI MS via flow injection at a mobile phase flow rate of 20 μl/min. Water/acetonitrile (1 : 1) was used as the mobile phase. ESI MS was performed in the positive mode with a spray voltage of 4.5 kV. The sheath gas flow rate was 40 ml/min and the capillary temperature 275° C.

RESULTS AND DISCUSSION

MALDI TOF MS analysis of C_3-symmetrical disks and their precursors

In this section, two matrixes (CHCA and DCTB) were employed for all the compounds. CHCA is one of the most widely used MALDI matrixes, and DCTB[28,29] is a nonprotic matrix that has demonstrated good performance for some labile samples. According to their structures (Fig. 1) and stages in the synthesis, the compounds studied here were arbitrarily divided into four groups: trialkoxy anilines (TAAs), oligopeptide anilides (OPAs), Boc-protection OPAs (Boc-OPAs) and C_3-symmetrical disks (SDs). The values of IP, proton affinity (PA) and pK_a of CHCA are listed in Table 1. Unfortunately, these values are not available for DCTB and for the SDs and their precursors. In Table 1, the values of reference compound, aniline, are also given. Some qualitative information for the analytes could be deduced by comparing their structures with that of aniline. For example, the IP values of the TAAs should be lower than that of aniline because of the conjugation through the substitution groups.

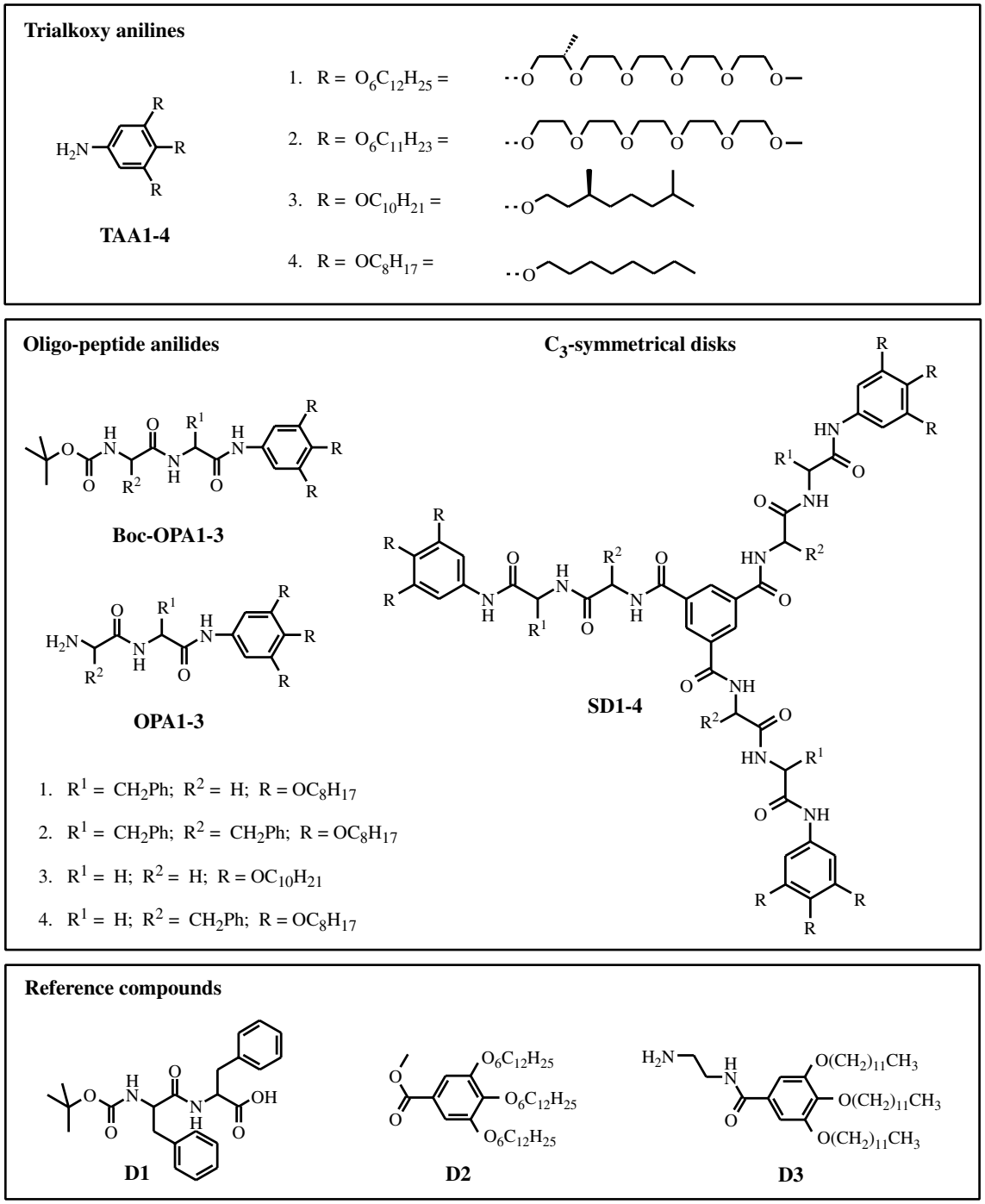

Figure 1. Structures of the C_3-symmetrical disks and their precursors.

Table 1. Values of ionization potential (IP), proton affinity (PA) and p*K* of CHCA and aniline[a]

	IP (eV)	PA (kJ/mol)	p*K*
CHCA	9.41	841	2.6 (pK_a)
Aniline	7.70	884	9.3 (pK_b)

[a] The IP values were taken from Refs 30 and 33; the PA values from Ref. 31; and p*K* values from Refs 32 and 34, respectively.

It should also be pointed out here that the accuracy and applicability of the values might be open to question.[22]

For the TAAs good MALDI TOF MS spectra were obtained with both matrixes tested. Figure 2 shows some typical spectra using CHCA as the matrix. In Fig. 2, signals of the radical and alkali ion adducts can readily be identified. CHCA is an acidic matrix. With this matrix, the anilines should be protonated prior to laser irradiation. One would expect that the protonated species should be the major peaks in the MS spectra. In contrast, however, the protonated ion peaks were found to be much smaller than their corresponding radical ion peaks, which is evident by comparing the recorded spectra with the simulated ones. The reason for this will be discussed later in this article. Some typical MS spectra with DCTB are shown in Fig. 3.

JMS

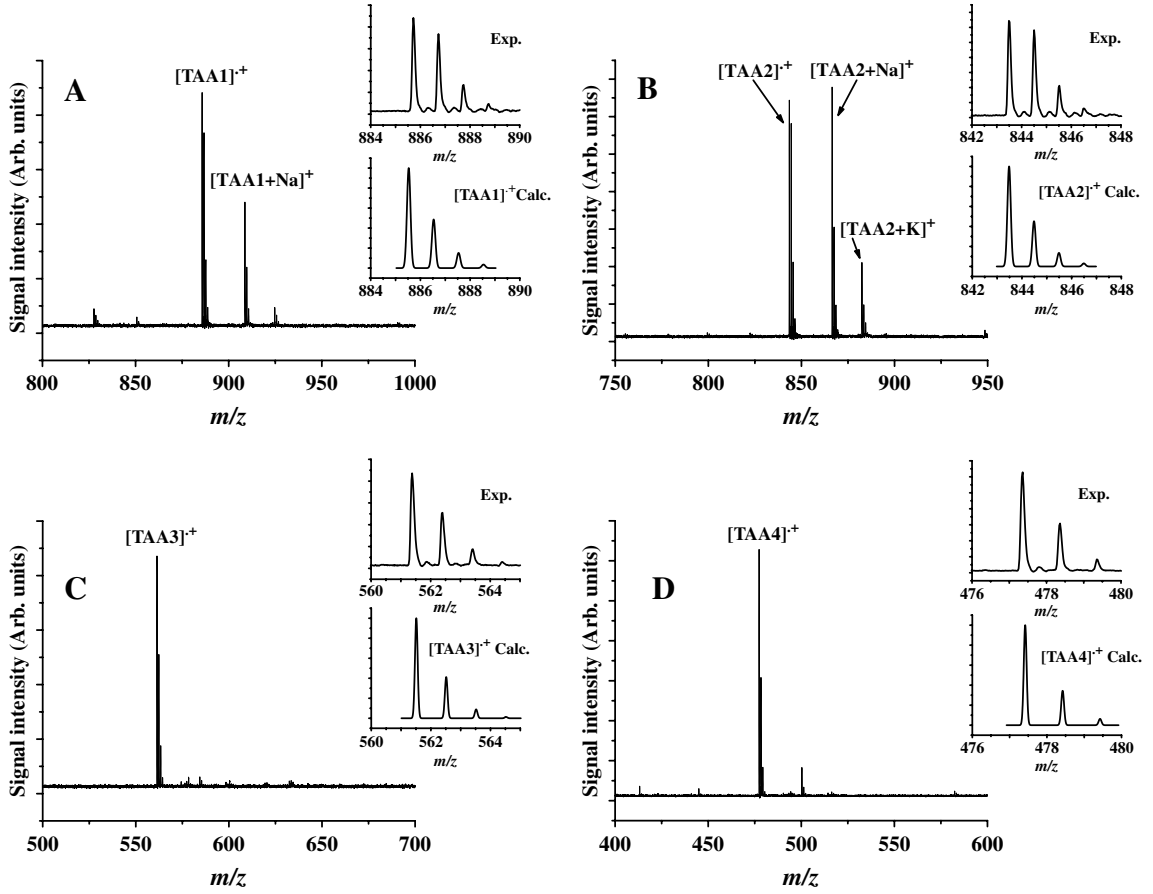

Figure 2. MALDI TOF MS spectra of the trialkoxy anilines using the CHCA matrix together with simulated spectra. (A) TAA1; (B) TAA2; (C) TAA3; (D) TAA4. The analyte structures are shown in Fig. 1.

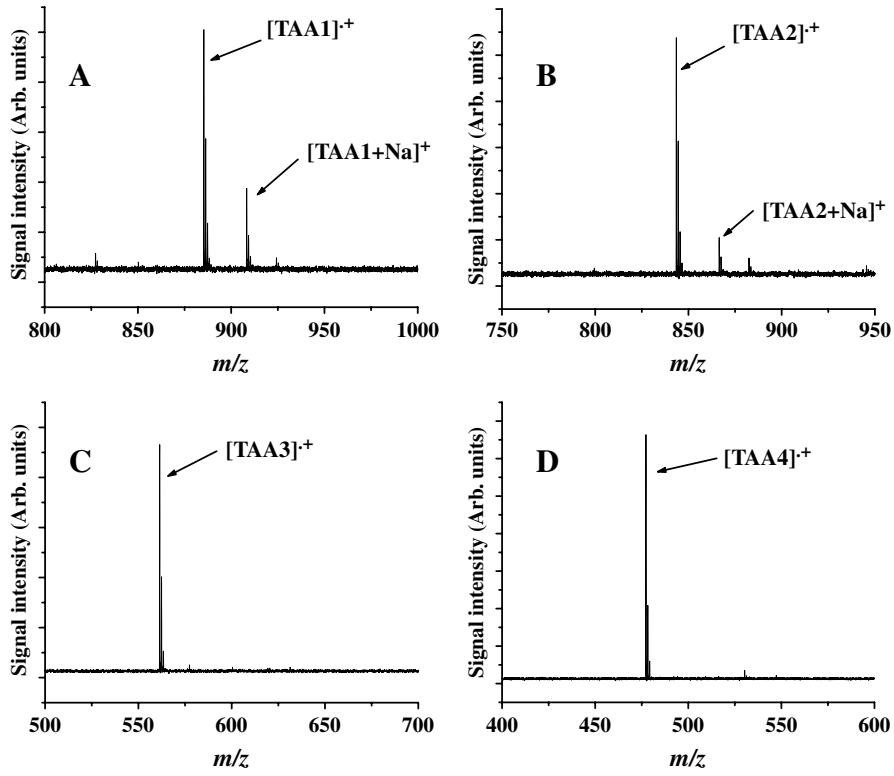

Figure 3. MALDI TOF MS spectra of the trialkoxy anilines with the DCTB matrix. (A) TAA1; (B) TAA2; (C) TAA3; (D) TAA4. The analyte structures are shown in Fig. 1.

As expected, with the nonacidic matrix, the protonated ion signals became much weaker or even negligible compared with the radical signals.

The (Boc)-OPAs are based on TAAs and different combinations of glycine (G) and phenylalanine (F) with and without Boc-protection of the amino group. Good MALDI TOF MS spectra were obtained with both CHCA and DCTB matrixes. Some typical spectra of the (Boc)-OPAs using the CHCA matrix are given in Fig. 4. Like for the TAAs, strong radical signals were also observed even for the OPAs, which contain free aliphatic amines that were not protected by the Boc-group.

For the SDs, three identical oligopeptides were attached onto a benzene-1,3,5-tricarbonyl core. Here again, good MALDI TOF MS spectra were obtained with both the matrixes tested. Some typical MS spectra of the disks using the CHCA matrix are given in Fig. 5. Clear radical ion peaks were observed for all the SDs.

In summary, good MS spectra were obtained for all the compounds tested. It can be concluded that MALDI TOF MS is a useful and straightforward method for the characterization of these compounds. One striking observation is that even with an acidic matrix, the free amines display prominent radical ion peaks. Protonated species, in contrast, were found to be more scarce or even negligible in the MALDI spectra. The peak intensities of radicals relative to their corresponding protonated molecules are listed in Table 2. The ratios were calculated on the basis of the theoretical isotopic distributions of the given molecules. By comparing the relative peak intensities of the mono-isotopic mass peak of $[A]^+$ and $[A + 1]^+$ in the experimental spectra with those of the theoretical values, the ratio of radicals to protonated ions can easily be calculated. The values listed in Table 2 must be regarded, however, as tentative since the signal intensities are not always very reproducible in MALDI. Nevertheless, it can clearly be seen that (1) with the acidic matrix (CHCA), protonated ions were observed only for compounds containing free amines (TAAs 1–4 and OPAs 1–3), and even under these circumstances the radical ions were more abundant than their protonated counterparts; (2) with the nonprotic matrix (DCTB), protonated ions were found to be negligible for all the compounds; and (3) for

Table 2. Intensity ratios between the analyte radical cation and the protonated ion ($[A]^+/[A + H]^+$) with the CHCA and DCTB matrixes

Trialkoxy anilines (TAAs)						
	TAA1	TAA2	TAA3	TAA4		
CHCA	3.2	2.5	6.8	6.9		
DCTB	–[a]	–	–	–		
Oligopeptide anilides (OPAs and Boc-OPAs)						
	OPA1	OPA2	OPA3	BocOPA1	BocOPA2	BocOPA3
CHCA	6.1	5.7	1.2	–	–	–
DCTB	–	–	–	–	–	–
C_3-symmetrical disks (SDs)						
	SD1	SD2	SD3	SD4		
CHCA	–	–	–	–		
DCTB	–	–	–	–		

[a] Strong analyte radical cations and negligible protonated analyte ions.

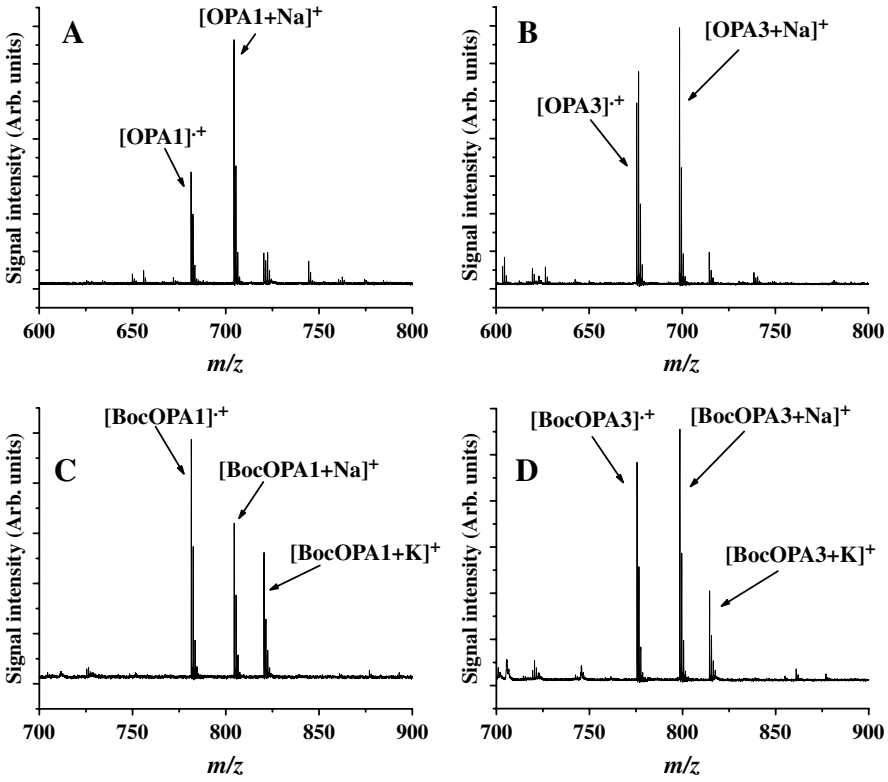

Figure 4. MALDI TOF MS spectra of oligopeptides with trialkoxy anilide end group using the CHCA matrix. (A) OPA1; (B) OPA3; (C) BocOPA1; (D) BocOPA3. The analyte structures are shown in Fig. 1.

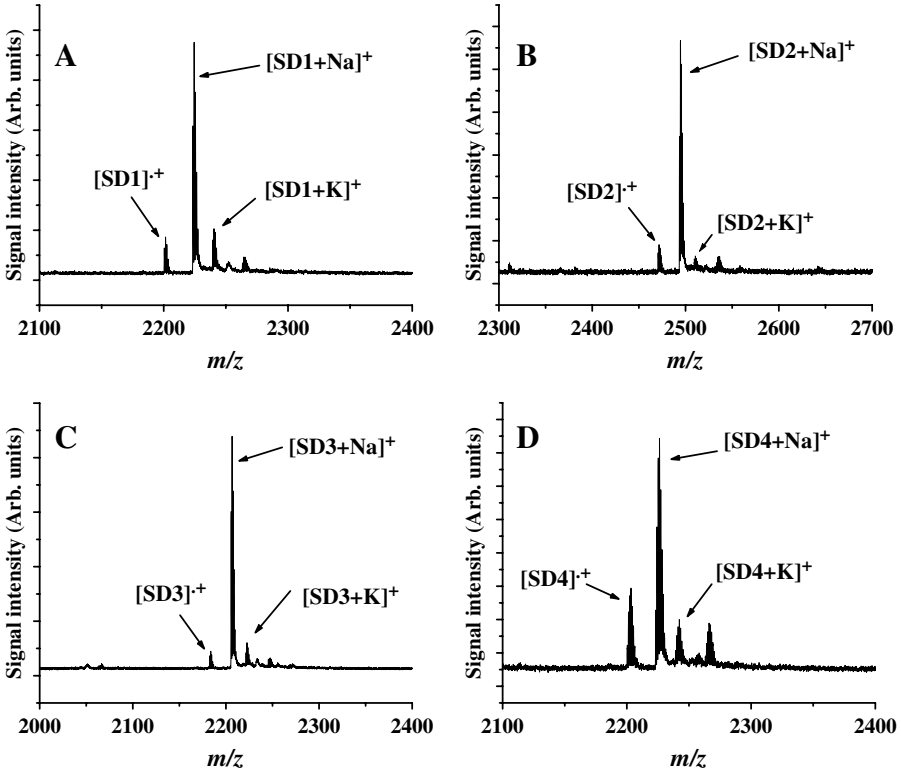

Figure 5. MALDI TOF MS spectra of the C_3-symmetrical disks with the CHCA matrix. (A) SD1; (B) SD2; (C) SD3; (D) SD4. The analyte structures are shown in Fig. 1.

compounds without a free amine (Boc-OPAs 1–3 and SDs 1–4), no significant amount of protonated ions were observed with either matrix tested. Contrary to the protonated ions, clear radical cation peaks were recorded in all experiments. Some possible mechanisms for the formation of radical ions will be discussed in the following section.

POSSIBLE MECHANISMS OF RADICAL CATION FORMATION

In the previous section, the observation of strong radical cation peaks in MALDI TOF MS of the C_3-symmetrical disks and their precursors has been discussed. Apart from the trialkoxy aniline/anilide moiety, the structures of the compounds are quite different (Fig. 1). Therefore, the formation of radical ions must, at least partly, be related with the aniline/anilide group. This inference was further supported by the MALDI TOF MS analysis of FFBoc (Fig. 1, D1), which is one of the small peptides used to make our OPAs by combining with trialkoxyaniline. It has been demonstrated above that OPAs showed strong radical signals. However, without the anilide group, FFBoc gave no radical ions. This suggests that radicals are indeed formed via the aniline/anilide group. Moreover, for the compounds in which the NH_2 group was replaced by, for example, carbonyl derivatives (compounds D2 and D3 in Fig. 1), no clear radical ions were detected either. Therefore, it can be concluded that the aniline/anilide group is essential for the radical ion formation. The radical ions are most likely developed by the loss of one electron from the N-atom and then stabilized by delocalization through the benzene ring. The MS spectra of compounds D1, D2 and D3 with the CHCA matrix are shown in Fig. 6.

Although both aniline and anilide groups could lead to the generation of radical ions, they exhibit significantly different ability to yield protonated ions, which is evident by comparing the ionization behaviors of TAAs and Boc-OPAs. When CHCA was used as the matrix, clear protonated ions, though considerably weaker than their corresponding radical ions, were observed for the TAAs. In contrast, however, protonated ions were found to be negligible for the Boc-OPAs (Table 2). The dramatic difference between these two types of compounds can be explained by studying the stability of the radical ions formed and the basicity of the molecules. Compared with the TAA radicals, the Boc-OPA radicals are more stable. This is because in addition to conjugation through the aromatic ring, the Boc-OPA radicals initiated by losing one electron from the anilide nitrogen are further stabilized by conjugation through the nearby carbonyl. Furthermore, the basicity of the Boc-OPAs is much weaker than that of the TAAs. The combined effects of stable radical and weak basicity result in the lack of protonated ions for the Boc-OPAs. With similar reasoning, the absence or presence of protonated ions for the other two series of samples studied (SDs and OPAs) could also be understood. Obviously, no protonated ions were observed for the SDs, which contain three oligopeptide anilides attached to a benzene-1,3,5-triscarboxamide core. The SD radical ions can be stabilized at least as well as the Boc-OPAs. For the OPAs, on the other hand, protonated ions were detected because of the presence of free aliphatic amines in the molecule. In the following experiments, efforts were mainly focused on

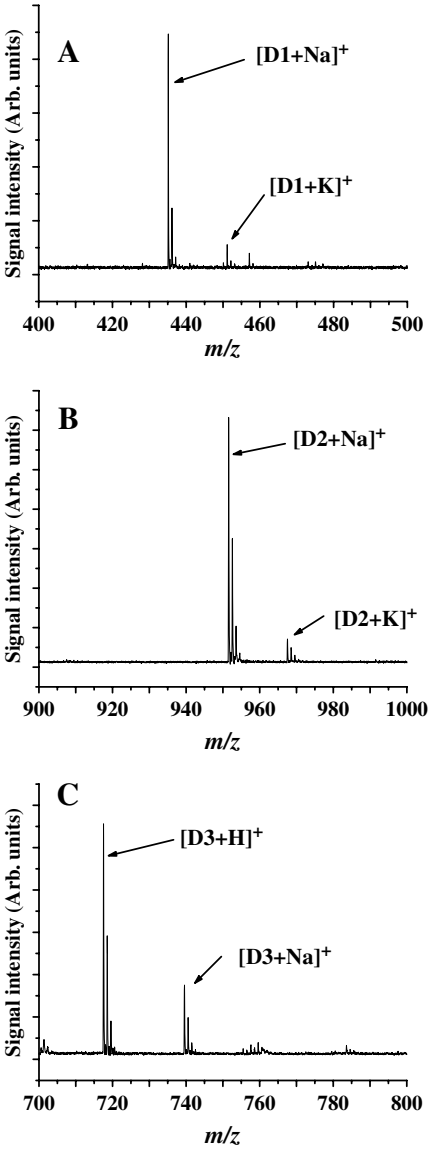

Figure 6. MALDI TOF MS spectra of D1, D2 and D3 with the CHCA matrix. (A) D1; (B) D2; (C) D3. The analyte structures are shown in Fig. 1.

the TAAs. This is because TAAs have the simplest structures among the four groups of compounds (Fig. 1), and could yield clear ions of both protonated and radical ion species. Protonated ions were found to be useful and could serve as references in the study of effects of the various experimental parameters on the generation of radical ions.

In the condensed phase with an acidic matrix, the TAAs should be protonated prior to laser irradiation. Direct measurements of some MALDI solutions (sample mixed together with the CHCA matrix) with ESI MS clearly show strong protonated ions. An ESI MS spectrum of TAA1 is shown in Fig. 7. From the ESI measurements, the following two conclusions can be drawn: (1) protonated trialkoxyaniline ions are stable under MS conditions; and (2) the formation of trialkoxyaniline radical ions is due to the MALDI process.

In order to find out whether the radical ions are formed by the electron-transfer reaction between neutral

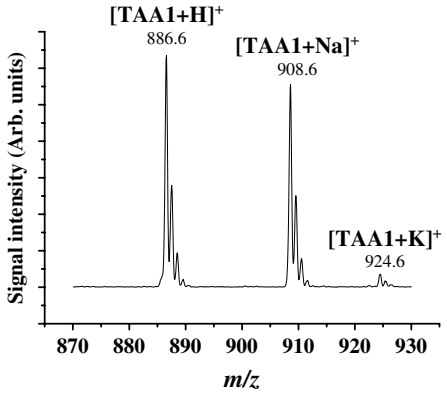

Figure 7. ESI MS spectrum of compound TAA1. The analyte structure is shown in Fig. 1.

Table 3. Effects of radical scavenger addition on the ion intensity ratios between analyte radical cation and protonated ion ($[A]^{\bullet+}/[A+H]^{+}$) with the CHCA matrix

Compounds	TAA1	TAA2	TAA3	TAA4
No scavenger	3.2	2.5	6.8	6.9
With BHT	3.4	2.8	6.7	6.9
With NTPBDA[a]	1.9	0.75	2.0	1.6

[a] *N*, *N*, *N*′,*N*′-tetraphenyl-1,4-benzenediamine.

analytes and matrix radical ions, the MALDI samples were mixed with a concentrated radical scavenger solution. The addition of excessive amounts of radical scavenger would quench the electron-transfer reaction between the analyte molecules and the matrix radicals. As a result, the radical ion peaks should disappear completely or at least become much weaker. In this study, BHT and NTPBDA were selected as the scavengers. BHT is a widely used antioxidant radical scavenger,[35,36] and NTPBDA is a compound with an extremely low IP value.[37] Surprisingly, no considerable influence was observed on the formation of analyte radicals with the addition of a far excessive amount of BHT, e.g. at a mole ratio of about 50 : 50 : 1 (matrix : BHT : analyte). For all the compounds tested, strong radical ion signals could still be observed (Fig. 8). Moreover, the $[A]^{\bullet+}/[A+H]^{+}$ ratio of the anilines remained literally unchanged (Table 3). Somewhat different results were obtained with NTPBDA. As expected, the analyte ion signals, including the alkali ion adducts, were significantly suppressed by the excessive amount of NTPBDA, which is very easy to be ionized. However, analyte radical ions could still be clearly observed. Comparison of the data listed in Table 3 shows that the $[A]^{\bullet+}/[A+H]^{+}$ ratios are slightly lower with the addition of NTPBDA. However, this should not be interpreted as a support for the electron-transfer mechanism because, otherwise, the ratio should be much lower or the aniline radicals should even have disappeared completely. The lower ratios might be explained by electron-transfer between the analyte radical and the NTPBDA scavenger with a lower IP value. Furthermore, on the basis of the electron-transfer mechanism alone, it is difficult to explain why only small peaks were observed for protonated ions that were already preformed with an acidic

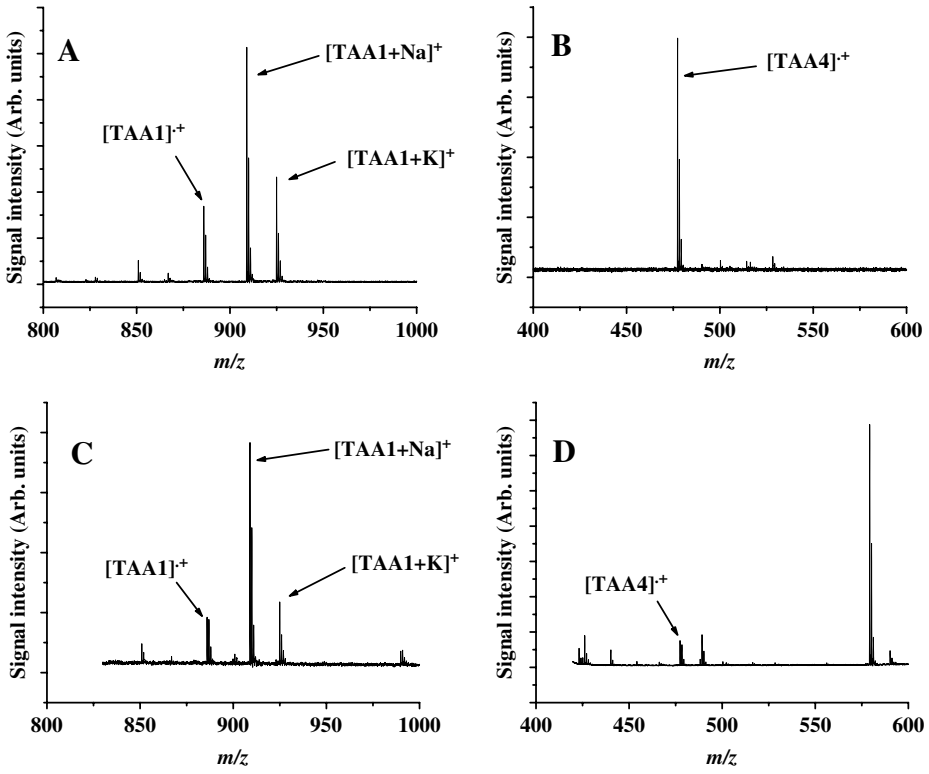

Figure 8. MALDI TOF MS spectra of TAA1 and TAA4 with the addition of radical scavengers. CHCA was used as the matrix. The mole ratio of matrix/scavenger/analyte is at about 50/50/1. (A) TAA1 with BHT; (B) TAA4 with BHT; (C) TAA1 with NTPBDA; (D) TAA2 with NTPBDA. The analyte structures are shown in Fig. 1.

matrix. From the results above, it appears that there are some other mechanisms responsible for the radical ion formation.

A possible route for the analyte radical ion formation is the direct photo-ionization upon laser irradiation. The anilines should have lower IP values than the matrixes used. Otherwise, no strong radical ion peaks would be detected since radicals of an analyte with high IP could not survive the collision with the neutral matrix molecules in the gas-phase plume. However, direct LDI of the anilines yielded no ions when conditions identical to those employed in MALDI were used. Much higher laser power is required in LDI to yield detectable ions. It is arguable that the analytes might be photoionized but difficult to be desorbed without matrix assistance. A matrix might provide a good environment facilitating the radical ion desorption. Anyway, on the basis of the dramatic difference between the results obtained by LDI and MALDI, it is evident that the matrix plays a crucial role for the radical ion formation/desorption of the TAAs.

In MALDI, a matrix absorbs laser energy and transfers most of it into thermal energy. Because of the low thermal conductivity of the organic solids, a huge temperature increase can be attained, which may play a key role in the various processes following the laser adsorption.[38] The surface peak temperature of MALDI matrixes under laser irradiation is normally around 1000 K.[38,39] For some compounds, the shortage of photon energy for direct photo-ionization might be compensated for by the thermal energy of the hot MALDI plume. Allwood *et al.*[40,41] developed a model based on thermal emission of electrons from photo-excited molecules for the formation of radical matrix ions. They claimed that this process might also be a plausible route for matrix ionization in MALDI.

$$2[Matrix]^* \xrightarrow{\Delta H} [Matrix]^{\bullet+} + [Matrix]^{\bullet-} \quad (1)$$

The anilines studied here have low IP values.[33,42,43] It is reasonable to assume that not only the matrix molecules but also the anilines could be ionized through the photo/thermal mechanism.

$$[Analyte]^* \xrightarrow{\Delta H} [Analyte]^{\bullet+} + e \quad (2)$$

For a given compound, whether a radical ion could be formed through photo- or photo/thermal ionization depends on its IP value. Unfortunately, the actual IP values in solid crystals or large matrix aggregates are still largely unknown.[22]

Supporting evidence for the photo-ionization mechanism was also found by two more series of independent experiments. In the first series, the trialkoxyanilines were studied with an inorganic particle matrix (ZnO) and with direct LDI. Clear radical ions could be observed in both cases. Some typical MS spectra are shown in Fig. 9. It should be noted that significantly higher laser intensities were required with ZnO or in LDI than that with a normal organic matrix. Evidently, with the inorganic matrix or in LDI, the radical ion formation could not occur through electron-transfer by molecule–ion reactions between neutral analytes and matrix radicals.

In the second series of experiments, excessive amount of K_2CO_3 was added as the cationization reagent (K_2CO_3/analyte at about 5/1 (mole/mole)). Figure 10 shows some

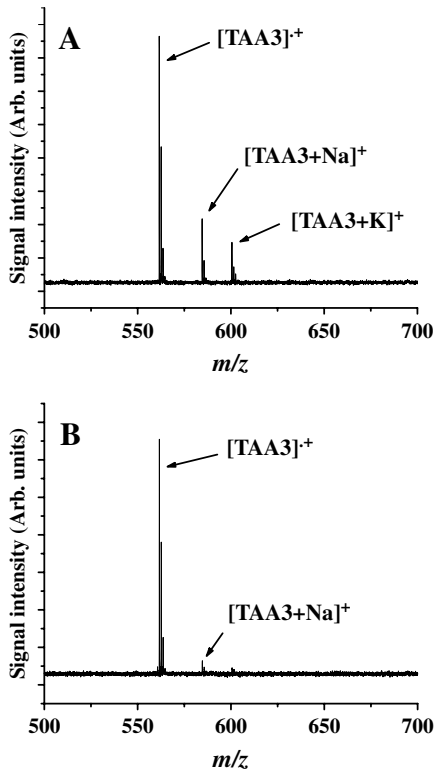

Figure 9. MS spectra of TAA3 with ZnO matrix and LDI. (A) LDI; (B) with ZnO matrix. The analyte structure is shown in Fig. 1.

typical MALDI TOF MS spectra with the addition of K_2CO_3. Although radical ions, and sodium and potassium adducts could be observed without the addition of any cationization reagent, the main goal of these experiments was to see how the generation of the radical ion and sodium adduct would be affected by adding K_2CO_3. In the literature, the formation of cation adducts was generally assumed and also demonstrated to be mainly through gas-phase reactions.[22–25,44] Because of the excessive amount of K^+ introduced, gas-phase reactions other than K^+ adduction would be suppressed. Indeed, by comparing Fig. 10 with Figs 2, 4 and 5, it is clear that the sodium adduct cation peaks, which were originally much more intensive than their corresponding potassium adduct peaks, almost completely disappeared. If the radical ions had also been formed in the gas-phase through molecule–ion reactions, their formation should be greatly suppressed too. Contrarily, however, radical cation signals could still be observed clearly. In compound SD2, for example, the Na^+ adduct peak was far stronger than the radical ion peak without the addition of K^+ (Fig. 5(B)). After the addition of K^+, the sodium adduct peak had completely disappeared while the radical cation could still be observed clearly (Fig. 10(C)). The results suggest that radical ions might already be formed through photo- or photo/thermal ionization prior to the plume reactions.

By using the photo- or photo/thermal ionization mechanism, the weakening of protonated ion peaks could also be reasonably explained. It is widely recognized that generation of ions in MALDI is a competing process. For the anilines with an acidic matrix, the protonated species were already preformed prior to laser irradiation, and intensive protonated

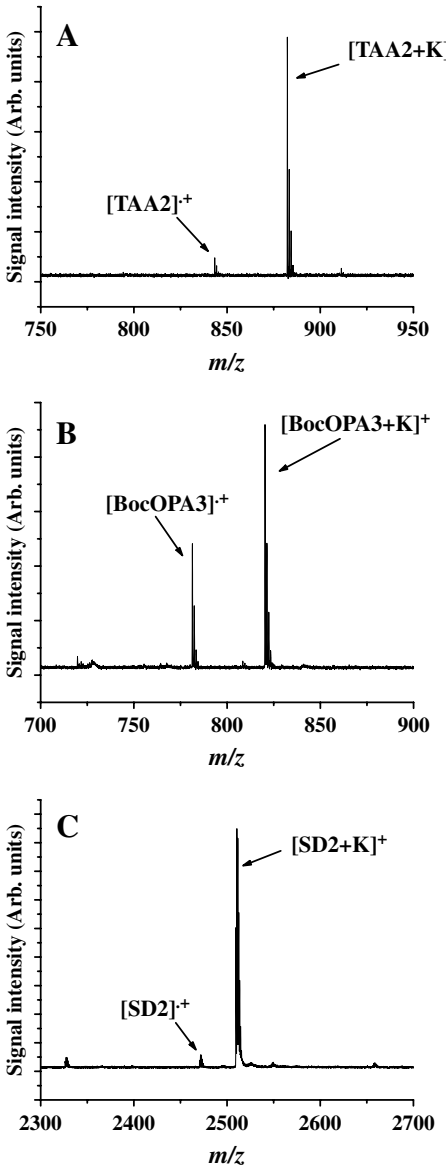

Figure 10. Typical MALDI TOF MS spectra with the addition of potassium carbonate. CHCA was used as the matrix. The mole ratio of matrix/K^+/analyte is at about 50/5/1. (A) TAA2; (B) BocOPA3; (C) SD2. The analyte structures are shown in Fig. 1.

ion peaks should be expected as in the case of many compounds containing an amino group. Contrarily, however, the protonated ion peaks were found to be quite small. This is probably due to the radical ion formation through photo- or photo/thermal ionization. Obviously, releasing of anilines as protonated ions straight from the condensed phase would be significantly suppressed when the analyte molecules had already been photo- or photo/thermally ionized as radical cations.

In addition to CHCA and DCTB, two more matrixes were studied. These were DHB and dithranol. CHCA and DHB are acidic, while DCTB and dithranol are more or less neutral. In order to neutralize the effects of matrix acidity, a large amount of succinic acid was added in the MALDI sample. Typical mole ratios of matrix : succinic acid : analyte were around 50 : 100 : 1. After the addition of succinic acid,

the final pH values of the MALDI solutions with different matrixes should be similar. Figure 11 shows some typical MS spectra of TAA2 with these matrixes. Similar results were obtained with other TAAs. Although the MALDI spot became less homogeneous after the addition of succinic acid, for a given compound the ratio of $[A]^{\bullet+}/[A + H]^+$ can be quite different with a different matrix. CHCA gave the highest ratio, presumably due to its 'hotter' nature compared with DHB and dithranol.[45,46] The results indicate that a hot matrix might favor the formation/desorption of analyte radical ions.

Judged from the results illustrated above, it seems that photo-ionization or photo/thermal ionization is a vital route for the radical ion formation of the compounds studied. This mechanism might also be applicable to other molecules with low IP values. However, it should be emphasized here that besides the radical ions, protonated and cationized pseudomolecular ions were also observed. The isotopic patterns of Na^+ and K^+ adducts were found to be fully compatible with their corresponding theoretical distributions. Apparently, ionization in MALDI is a very complicated process that might involve several different ionization mechanisms.

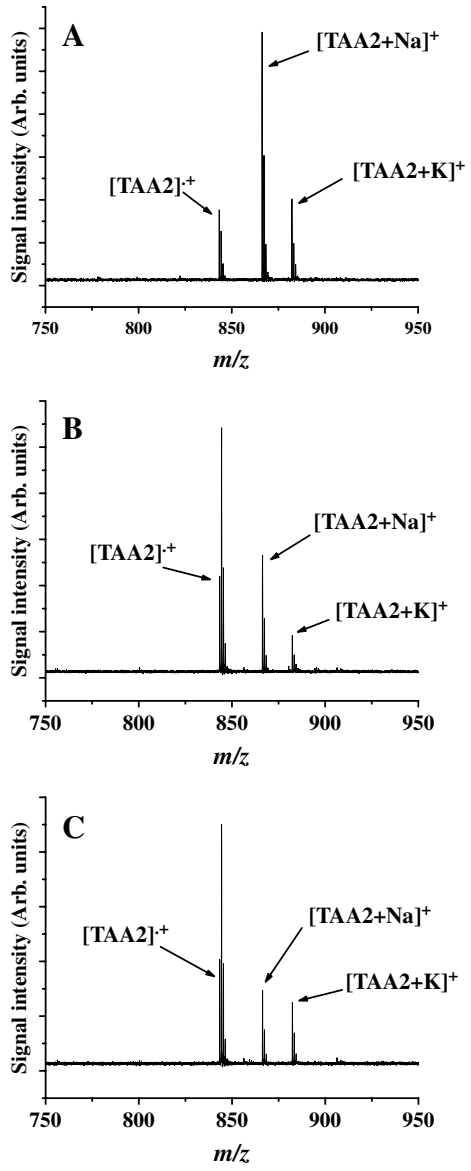

Figure 11. Comparison of MALDI TOF MS spectra of TAA2 using different matrixes with the addition of succinic acid. The mole ratio of matrix/succinic acid/analyte is at about 50/100/1. (A) CHCA; (B) DHB; (C) dithranol. The analyte structure is shown in Fig. 1.

CONCLUSIONS

MALDI TOF MS is a powerful and straightforward technique for the characterization of novel C_3-symmetrical tris(dipeptide) disks and their precursors. For all the compounds tested, radical ion peaks and cationized pseudomolecular ion peaks could readily be identified. The radicals were probably formed by losing one electron from the aniline/anilide nitrogen and stabilized by conjugation through the phenyl ring. It appears that direct ionization of the analytes by a photo- or photo/thermal mechanism is an important route for the radical ion formation. Important roles of the matrix for the generation of radical ions might include providing a good environment for desorption and making up the energy difference between photon excitation and analyte IP.

Acknowledgements

The authors are grateful to Dr M. M. Wienk and Prof. R. A. J. Janssen for their helpful discussions. Dr M. M. Wienk is further acknowledged for kindly providing NTPBDA. We also thank Dr S. Langereis for transferring all the figures into the EPS format.

REFERENCES

1. van Gorp JJ, Vekemans JAJM, Meijer EW. C_3-symmetric supramolecular architectures: fibers and organic gels from discotic trisamides and trisureas. *J. Am. Chem. Soc.* 2002; **124**: 14759.
2. Brunsveld L, Schenning APHJ, Broeren MAC, Janssen HM, Vekemans JAJM, Meijer EW. Chiral amplification in columns of self-assembled N,N′,N′′-tris[(S)-3,7-dimethyloctyl]benzene-1,3,5-tricarboxamide in dilute solution. *Chem. Lett.* 2000; 292.
3. Palmans ARA, Vekemans JAJM, Hikmet RA, Fisher H, Meijer EW. Lyotropic liquid-crystalline behavior in disc-shaped compounds incorporating the 3,3′-di(acylamino)-2,2′-bipyridine unit. *Adv. Mater.* 1998; **10**: 873.
4. Palmans ARA, Vekemans JAJM, Havinga EE, Meijer EW. Sergeants-and-soldiers principle in chiral columnar stacks of disk-shaped molecules with C3 symmetry. *Angew. Chem., Int. Ed. Engl.* 1997; **36**: 2648.
5. Brunsveld L, Zhang H, Glasbeek M, Vekemans JAJM, Meijer EW. Hierarchical growth of chiral self-assembled structures in protic media. *J. Am. Chem. Soc.* 2000; **122**: 6175.
6. Brunsveld L, Folmer BJB, Meijer EW, Sijbesma RP. Supramolecular polymers. *Chem. Rev.* 2001; **101**: 4071.
7. Mateos-Timoneda MA, Crego-Calama M, Reinhoudt DN. Supramolecular chirality of self-assembled systems in solution. *Chem. Soc. Rev.* 2004; **33**: 363.
8. van Bommel KJC, van der Pol C, Muizebelt I, Friggeri A, Heeres A, Meetsma A, Feringa BL, van Esch J. Responsive cyclohexane-based low-molecular-weight hydrogelators with modular architecture. *Angew. Chem., Int. Ed. Engl.* 2004; **43**: 1663.
9. Cole RB (ed). *Electrospray Ionization Mass Spectrometry: Fundamentals, Instrumentation, and Applications*. John Wiley and Sons: New York, 1997.

10. Yamashita M, Fenn JB. Electrospray ion source. Another variation on the free-jet theme. *J. Phys. Chem.* 1984; **88**: 4451.
11. Karas M, Bachmann D, Bahr U, Hillenkamp F. Matrix-assisted ultraviolet laser desorption of non-volatile compounds. *Int. J. Mass Spectrom. Ion Processes* 1987; **78**: 53.
12. Tanaka K, Waki H, Ido Y, Akita S, Yoshida Y, Yoshida T. Protein and polymer analyses up to m/z 100 000 by laser ionization time-of-flight mass spectrometry. *Rapid Commun. Mass Spectrom.* 1988; **2**: 151.
13. Burlingame AL, Boyd RK, Gaskell SJ. Mass spectrometry. *Anal. Chem.* 1998; **70**: 647R.
14. Nielen MWF. MALDI time-of-flight mass spectrometry of synthetic polymers. *Mass Spectrom. Rev.* 1999; **18**: 309.
15. Farmer TB, Caprioli RM. Determination of protein-protein interactions by matrix-assisted laser desorption/ionization mass spectrometry. *J. Mass Spectrom.* 1998; **33**: 697.
16. Juhasz P, Costello CE. Generation of large radical ions from oligometallocenes by matrix-assisted laser desorption/ionization. *Rapid Commun. Mass Spectrom.* 1993; **7**: 343.
17. McCarley TD, McCarley RL, Limbach PA. Electron-transfer ionization in matrix-assisted laser desorption/ionization mass spectrometry. *Anal. Chem.* 1998; **70**: 4376.
18. Ehring H, Karas M, Hillenkamp F. Role of photoionization and photochemistry in ionization processes of organic molecules and relevance for matrix-assisted laser desorption ionization mass spectrometry. *Org. Mass Spectrom.* 1992; **27**: 472.
19. Lidgard RO, McConnell DB, Black DSC, Kumar N, Duncan MW. Fragmentation observed in continuous extraction linear MALDI: a cautionary note. *J. Mass Spectrom.* 1996; **31**: 1443.
20. Rader HJ, Spickermann J, Kreyenschmidt M, Mullen K. MALDI-TOF mass spectrometry in polymer analysis, molecular weight analysis of rigid rod polymers. *Macromol. Chem. Phys.* 1996; **197**: 3285.
21. Green MK, Medforth CJ, Muzzi CM, Nurco DJ, Shea KM, Smith KM, Lebrilla CB, Shelnutt JA. Application of matrix-assisted laser desorption fourier transfer mass spectrometry to the analysis of planar porphyrins and highly substituted nonplanar porphyrins. *Eur. Mass Spectrom.* 1997; **3**: 439.
22. Zenobi R, Knochenmuss R. Ion formation in MALDI mass spectrometry. *Mass Spectrom. Rev.* 1998; **17**: 337.
23. Karas M, Gluckmann M, Schafer J. Ionization in matrix-assisted laser desorption/ionization: singly charged molecule ions are the lucky survivors. *J. Mass Spectrom.* 2000; **35**: 1.
24. Knochenmuss R, Zenobi R. MALDI ionization: the role of in-plume processes. *Chem. Rev.* 2003; **103**: 441.
25. Karas M, Kruger R. Ion formation in MALDI: the cluster ionization mechanism. *Chem. Rev.* 2003; **103**: 427.
26. Miller TM, Kwock EW, Neenan TX. Synthesis of four generations of monodisperse aryl ester dendrimers based on 1,3,5-benzenetricarboxylic acid. *Macromolecules* 1992; **25**: 3143.
27. Sinkeldam RW, van Houtem MHCJ, Vekemans JAJM, Meijer EW. Synthesis of 3,6-diaminophthalimides for ureidophthalimide-based foldamers. *Org. Lett.* 2006; **8**: 383.
28. Ulmer L, Torres-Gacia HG, Mattay J, Luftmann H. The use of 2-[(2E)-3-(4-*tert*-butylphenyl)-2-methylprop-2-enylidene] malononitrile as matrix for matrix-assisted laser desorption/ionization mass spectrometry. *Eur. J. Mass Spectrom.* 2000; **6**: 49.
29. Lou X, van Buijtenen J, Bastiaansen JJAM, de Waal BFM, Langeveld BMW, van Dongen JLJ. Characterization of some synthetic Ru and Ir complexes by matrix-assisted laser desorption/ionization time-of-flight mass spectrometry. *J. Mass Spectrom.* 2005; **40**: 654.
30. Sumner LW, Huang Y, Russell DH. MALDI internal energy transfer studies utilizing molecular modeling. *Proceedings of the 44th ASMS Conference on Mass Spectrometry*, Portland, 1996; 271.
31. Jorgensen TJD, Bojesen G, Rahbek-Nielsen H. The proton affinities of seven matrix-assisted laser desorption/ionization matrices correlated with the formation of multiply charged ions. *Eur. Mass Spectrom.* 1998; **4**: 39.
32. Sipila J, Nurmi H, Kaukonen AM, Hirvonen J, Taskinen J, Yli-Kauhaluoma J. A modification of the Hammett equation for predicting ionization constants of p-vinyl phenols. *Eur. J. Pharm. Sci.* 2005; **25**: 417.
33. Farrell PG, Newton J. Ionization potentials of aromatic amines. *J. Phys. Chem.* 1965; **10**: 3506.
34. Budavari S, O'Neill MJ, Smith A, Heckelman PE (eds). *The Merck Index*, 8th ed. Merck and Company: Rahway, NJ, 1989; 104.
35. Fujisawa S, Kadoma Y, Yokoe I. Radical scavenging activity of butylated hydroxytoluene (BHT) and its metabolites. *Chem. Phys. Lipids* 2004; **130**: 189.
36. Green TR, Bennett SR, Nelson VM. Specificity and properties of propofol as an antioxidant free radical scavenger. *Toxicol. Appl. Pharmacol.* 1994; **129**: 163.
37. Wienk MM. High-Spin molecules of phosphorus and nitrogen-centered radicals, Ph. D. Thesis, Technical University of Eindhoven, Eindhoven, 1997.
38. Koubenakis A, Frankevich V, Zhang J, Zenobi R. Time-resolved surface temperature measurement of MALDI matrices under pulsed UV laser irradiation. *J. Phys. Chem. A* 2004; **108**: 2405.
39. Mowry CD, Johnston MV. Internal energy of neutral molecules ejected by matrix-assisted laser desorption. *J. Phys. Chem.* 1994; **98**: 1904.
40. Allwood DA, Dyer PE, Dreyfus RW. Ionization modeling of matrix molecules in ultraviolet matrix-assisted laser desorption/ionization. *Rapid Commun. Mass Spectrom.* 1997; **11**: 499.
41. Allwood DA, Dyer PE, Dreyfus RW, Perera IK. Plasma modeling of UV matrix assisted laser desorption ionization (MALDI). *Appl. Surf. Sci.* 1997; **109/110**: 616.
42. Birks JB. *Photophysics of Aromatic Molecules*. Wiley: New York, 1970.
43. Ogawa T, Ogawa T, Nakashima K. Ionization of anilines in nonpolar hydrocarbon solvents as studied by two-photon ionization spectra. *J. Phys. Chem.* 1998; **102**: 10608.
44. Rashidezadeh H, Guo B. Investigation of metal attachment to polystyrenes in matrix-assisted laser desorption ionization. *J. Am. Soc. Mass Spectrom.* 1998; **9**: 724.
45. Juhasz P, Vestal ML, Martin SA. On the initial velocity of ions generated by matrix-assisted laser desorption ionization and its effects on the calibration of delayed extraction time-of-flight mass spectrometry. *J. Am. Soc. Mass Spectrom.* 1997; **8**: 209.
46. Gluckmann M, Karas M. The initial ion velocity and its dependence on matrix, analyte and preparation method in ultraviolet matrix-assisted laser desorption/ionization. *J. Mass Spectrom.* 1999; **34**: 467.